Radiation hardness of the Low Gain Avalanche Diodes developed by NDL and IHEP in China

Y.Y. Fan[a,c], S. Alderweireldt[d], C. Agapopoulou[e], N. Atanov[f], M. Kassem Ayoub[a], D. Caforio[g], H. Chen[h], S. Christie[i], J. G. da Costa[a], H. Cui[a,b], G. d'Amen[j], Y. Davydov[f], R. Kiuchi[a], A. S. C. Ferreira[d], Z. Galloway[i], M. Garau[k], L. C. García[l], J. Ge[h], C. Gee[i], G. Giacomini[j], V. Gkoukousis[l], C. Grieco[l], S. Guindon[d], D. Han[m], S. Han[a,b], Y. Huang[a], Y. Jin[i], M. Jing[a,b], E. Kuwertz[d], C. Labitan[i], M. Leite[n], H. Liang[h], Z. Liang[a,c,*], B. Liu[a], J. Liu[a], M. Lockerby[i], F. Lyu[a], N. Makovec[e], S. M. Mazza[i], F. Martinez-Mckinney[i], I. Nikolic[o], R. Padilla[i], B. Qi[a,b], K. Ran[a,b], H. Ren[i], C. Rizzi[d], E. Rossi[j], S. Sacerdoti[e], H. F.-W. Sadrozinski[i], G. T. Saito[n], B. Schumm[i], A. Seiden[i], L. Shan[a], L. Shi[a], Y. Tan[a,b], A. Tricoli[j], S. Trincaz-Duvoid[o], M. Wilder[i], K. Wu[a,b], W. Wyatt[i], X. Shi[a,c], T. Yang[a,b], Y. Yang[a], C. Yu[a,b], X. Zhang[m], L. Zhao[h], M. Zhao[a,c], Y. Zhao[i], Z. Zhao[h], X. Zheng[h], X. Zhuang[a]

[a] *Institute of High Energy Physics, Chinese Academy of Sciences, 19B Yuquan Road, Shijingshan District, Beijing 100049, China*
[b] *University of Chinese Academy of Sciences, 19A Yuquan Road, Shijingshan District, Beijing 100049, China*
[c] *State Key Laboratory of Particle Detection and Electronics, Institute of High Energy Physics, Chinese Academy of Sciences, Beijing 100049*
[d] *CERN, Esplanade des Particules 1, 1211 Geneva 23*
[e] *LAL, IN2P3-CNRS and Université Paris Sud, 91898 Orsay Cedex, France*
[f] *Joint Institute for Nuclear Research, Joliot-Curie street 6, Dubna, 141980 Russia*
[g] *Justus Liebig University Giessen, Ludwigstrasse 23, Giessen, Hesse 35390*
[h] *Department of Modern Physics and State Key Laboratory of Particle Detection and Electronics, University of Science and Technology of China, Hefei 230026, China*
[i] *SCIPP, Univ. of California Santa Cruz, CA 95064, USA*
[j] *Brookhaven National Laboratory (BNL), Upton , NY 11973, U.S.A.*
[k] *University of Cagliari, Via Universitá 40, Cagliari, Sardinia 09124*
[l] *Institut de Física d'Altes Energies (IFAE), Carrer Can Magrans s/n, Edifici Cn, Universitat Autónoma de Barcelona (UAB), E-08193 Bellaterra (Barcelona), Spain*
[m] *Novel Device Laboratory, Beijing Normal University, No. 19, Xinjiekouwai Street, Haidian District, Beiing 100875, China*
[n] *Instituto de Física - Universidade de São Paulo (USP), R. do Matão, 1371, Cidade Universitária, São Paulo - SP 05508-090 - Brazil*
[o] *LPNHE, Sorbonne Université, Université de Paris, CNRS/IN2P3, Paris; France*

*Corresponding author: Zhijun Liang (liangzj@ihep.ac.cn)

Preprint submitted to Nuclear Instruments and Methods in Physics Research Section AMarch 20, 2020

ATL-LARG-PROC-2020-005
20 March 2020

Abstract

This paper studied the radiation hardness of low gain avalanche detector (LGAD) developed by the Novel Device Laboratory (NDL) in Beijing and the Institute of High Energy Physics (IHEP) of Chinese Academy of Sciences, in the context of an upgrade project of the ATLAS detector for the high luminosity phase of LHC. NDL LGAD sensors with different layouts, epitaxial resistivity, doping profile were irradiated up to 1.02×10^{15} n_{eq}/cm^2 by 70 MeV proton at Cyclotron and Radioisotope Center (CYRIC). The timing resolution of NDL LGAD sensors reached 50 picoseconds (ps) and the collected charge reached 3 - 4 Femtocoulombs (fC) after irradiation.

Keywords: LGAD, proton irradiation, beta test, timing resolution, HGTD

1. Introduction

Low gain avalanche detector (LGAD) is one kind of ultra-fast silicon detector (UFSD), which is a thin n-on-p silicon sensor with an internal multiplication layer, as shown in Figure 1. Thin LGAD has high signal-to-noise ratio and short signal rise time. Therefore it has a very good timing resolution. LGAD could be applied in many aspects. One application of LGAD is the development of a high granularity timing detector (HGTD) [1] in the upgrade of the ATLAS experiment at the High Luminosity Large Hadron Collider (HL-LHC) [2]. In HGTD project, LGAD is required to reach 70 picoseconds (ps) timing resolution after an irradiation up to f 2.5×10^{15} n_{eq}/cm^2. The collected charge of LGAD is also required to be larger than 4 fC to reduce jitter in readout ASIC chip.

As Ref. [3, 4, 5] reported, the Centro Nacionalde Microelectronica (CNM) and Fondazione Bruno Kessler (FBK) and Hamamatsu Photonics (HPK) have achieved the timing resolution below 70 ps before irradiation. However, due to the high luminosity of the HL-LHC, LGADs will operate in conditions of very harsh irradiation and the timing resolution of LGADs degraded with increase of the neutron fluences due to the acceptor removal mechanism [5, 6, 7]. Several groups around the world are working on the improvement of the radiation hardness of LGAD. The Institute of High Energy Physics (IHEP) of the Chinese Academy of Science cooperated with Novel Device Laboratory (NDL) [8] on LGAD sensor development since 2019. Many irradiation studies

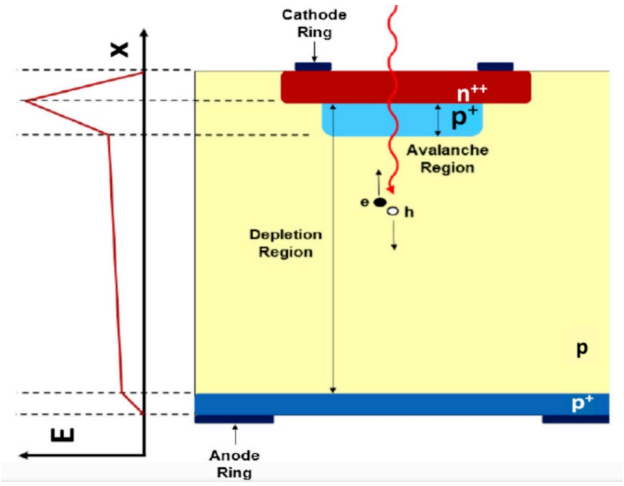

Figure 1: Shematic for the LGAD sensors.

have been performed for the HPK and CNM LGAD sensors [5, 6, 9, 10, 11], but the properties of NDL LGADs haven't been studied after proton irradiation. This paper studied the timing resolution and charge collection of NDL LGAD after proton irradiation up to 1.02×10^{15} n_{eq}/cm^2 at Cyclotron and Radioisotope Center (CYRIC) in Japan.

2. Introduction to NDL LGAD sensors

NDL LGAD sensors were designed by the NDL and IHEP, and were produced by a CMOS foundry. The LGAD sensor is fabricated on the p-type epitaxial layer of silicon substrate. The epitaxial layer is 33 µm thick with resistivity of $100\,\Omega \cdot$ cm or $300\,\Omega \cdot$ cm. The substrate on which the epitaxial layer is grown is heavily doped. It acts as an ohmic contact and mechanical support [8]. Two batches of the NDL LGADs with 2×2 pad array were tested in this study. NDL BV170 is one of the first batch, while NDL #9 and NDL #10 belong to the second batch. The thickness of the substrate for the first (second) batch is 300 (250) µm. BV170 is fabricated with a low-resistivity ($100\,\Omega \cdot$ cm) epitaxial layer, and it has six guard rings, as shown in Figure 2 (a). NDL #9 and NDL #10 are fabricated with high-resistivity ($300\,\Omega \cdot$ cm) epitaxial layer, and they have two guard rings as shown in Figure 2 (b). The guard rings of BV170 are without probing pad and they can only be floated. While the guard rings of NDL #9 and NDL #10 are with probing pads, and

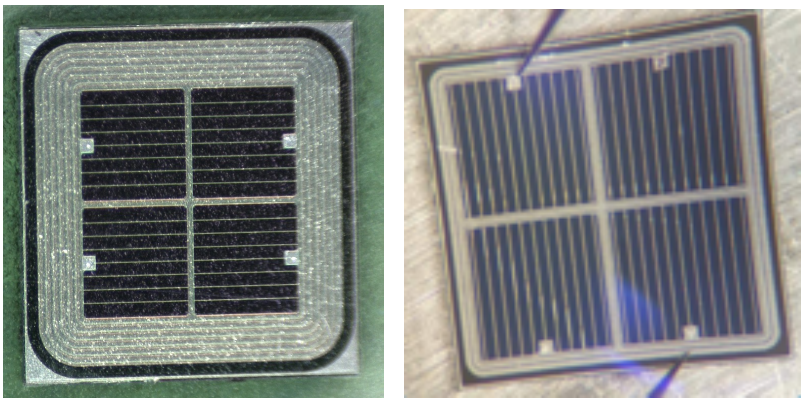

(a) (b)

Figure 2: (a) Photo of the first batch of NDL LGAD sensor (BV170). There are six guard rings in this batch. However, the guard rings are without probing pad. (b) Photo of of the second batch of NDL LGAD sensors (NDL #9 and NDL #10). Two guard rings designed are used in this batch.

Table 1: Properties of three type of IHEP-NDL LGAD sensors. The sensor breakdown voltage (V_{BD}), and depleted voltage ($V_{depleted}$), the dimension of one pad, the resistivity of wafer epitaxial layer (R_{epi}) and the gain value are summarized.

Batch	Sensor	Breakdown Voltage [V]	Depleted Voltage [V]	Pad Size [mm]	Wafer Resistance [$\Omega \cdot$ cm]	Gain
1^{st}	BV170	165	100	1×1	100	30
2^{ed}	#10	300	40	1.3×1.3	300	20
	#9	250	40	1.3×1.3	300	20

they can be either grounded or floated. The detailed parameters of NDL sensors are listed in the Table 1.

Figure 3 shows the inverse of capacitance square as a function of the biased voltage of the sensors at room temperature (20 °C). The full depletion voltages for NDL #10, NDL #9 and BV170 are 40 V, 40 V and 100 V, respectively. The punch-through voltages for the multiplication layer of the NDL #10, NDL #9 and BV170 are about 28 V, 28 V, and 20 V. The frequency of LCR meter in the test is 10 kHZ.

As Ref [12, 13] reported, the doping profile could be extracted from the capacitance-voltage (CV) measurement. The dependence of doping concentration (N_w) on depth (w) was obtained with the following equations:

$$N_w = -\frac{2}{q\epsilon_r\epsilon_0 A^2}[\frac{d}{dV}(\frac{1}{C^2})]^{-1} \quad (1)$$

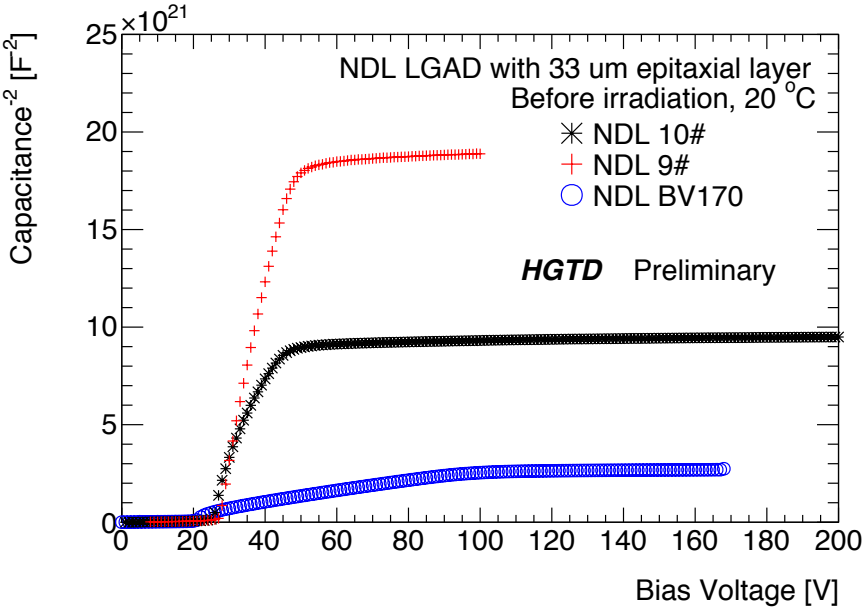

Figure 3: The inverse of capacitance square as a function of the biased voltage of NDL LGAD sensors.

with

$$w = \epsilon_r \epsilon_0 \frac{A}{C} \tag{2}$$

where q is the electron charge equal to 1.6×10^{19} fC, ϵ_r is the silicon relative permittivity equal to 11.7, ϵ_0 is the vacuum absolute permittivity equal to 8.854×10^{-14} fC/cm, A is the active area of the silicon sensor, C is the measured capacitance , V is the biased voltage. The Doping profile of NDL LGAD is shown in Figure 4. The depth of the multiplication layer is about 0.6 µm. The multiplication layer width in the first (second) batch is 0.5 µm (1 µm). The peak of doping concentration in the multiplication layer in the second batch is about two times lower than that of the first batch.

3. CYRIC irradiation

Three kinds of NDL LGAD sensors, which were BV170, NDL #9 and NDL #10, were irradiated up to 1.02×10^{15} n_{eq}/cm^2 at CYRIC in Japan with 70 MeV proton. The proton fluence was quoted in 1 MeV equivalent neutrons per cm^2.

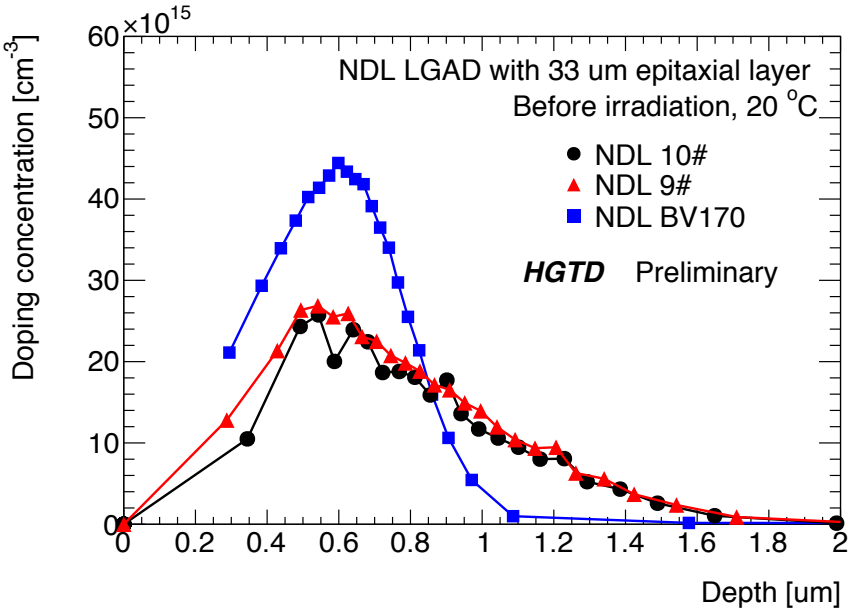

Figure 4: The doping profile of NDL LGAD sensors estimated from CV measurements.

After irradiation, the NDL LGAD sensors were annealed for 80 min at 60 °C, which roughly simulate the long-term annealing in the end-of-year shut-down period during the operation of the HL-LHC. After irradiation, the NDL LGAD sensors were shipped to other laboratories to be tested.

4. Experiment Setup

The readout board for NDL LGAD sensors was designed by the University of California Santa Cruz (UCSC), which had low noise and high bandwidth trans-impedance amplifiers. The readout board has been used in previous studies. Detailed description is in [3, 5].

Setup for beta test is shown in Figure 5. The detailed description for the setup is in [3, 5]. The beta tests were done by UCSC.The device under test (DUT) and the trigger were housed in the climate chamber. This can guarantee the temperature to be −30 °C, which is the operating temperature at the HL-LHC. The beta source was ^{90}Sr. The entire waveform of the DUT and trigger was recorded by the digital oscilloscope (2.5 GHz-8bit vertical resolution LeCroy WavePro 725Zi-A). After proton irradiation, the doping

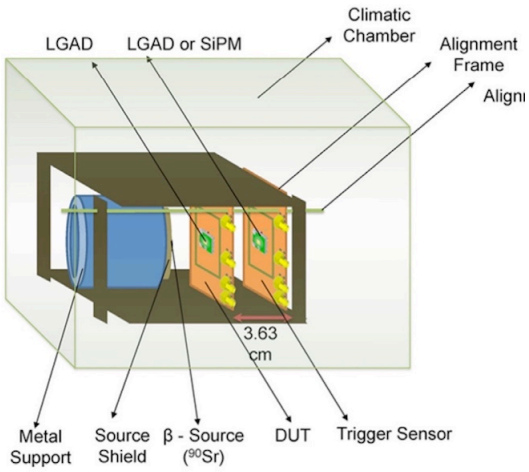

Figure 5: Beta test setup for the NDL sensors.

concentration of the gain layer decreases. To regain the performance of the unirradiated sensor, the bias voltage for the irradiated sensor should be increased. However, the bias voltage is tested only up to 500 V, since 500 V is a typical safe operating voltage for the LGAD with 33 µm thick epitaxial layer after irradiation.

4.1. Timing Resolution

The data of the beta test was analyzed offline according to [14]. The timing resolution θ_t can be evaluated as the following equation:

$$\theta_t^2 = \theta_{Jitter}^2 + \theta_{LandauNoise}^2 + \theta_{Distortion}^2 + \theta_{Timewalk}^2 \tag{3}$$

The θ_{Jitter}^2 depends on the signal to noise rate and the rising speed of the signal pulse. For NDL LGAD the epitaxial layer was thinned to 33 µm for reducing the signal rise time, the θ_{Jitter}^w and the $\theta_{LandauNoise}^2$. A moderate gain value (20 - 30) is chosen for increasing the signal to noise ratio while keeping a low shot noise. $\theta_{LandauNoise}^2$ is the fluctuations of the charge deposition in the LGAD. $\theta_{Distortion}^2$ is caused by the distortion of the electric field. The surface of NDL LGAD is covered by several Aluminum strips as shown in Figure 2. This layout of NDL LGAD sensor can generate a uniform electric field and also keep its sensitivity to light. $\theta_{Timewalk}^2$ is caused by time walk effect, in which small signal and large signal have different arrival time. The

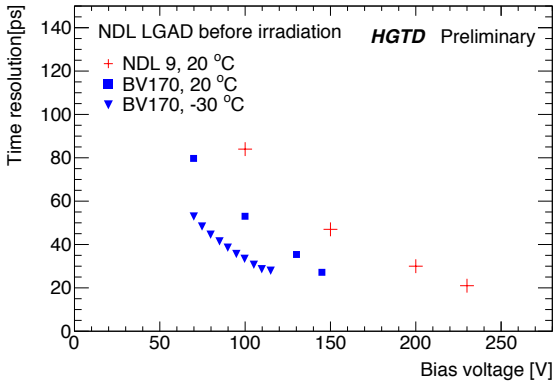

(a)

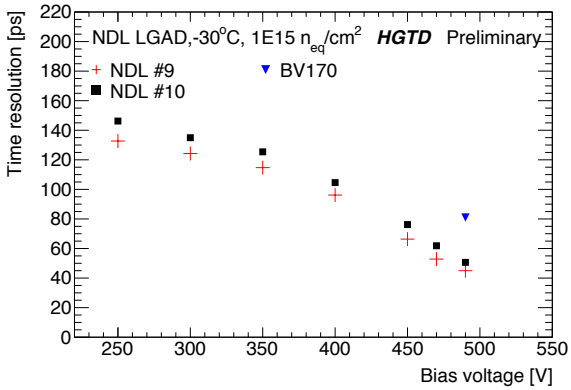

(b)

Figure 6: (a) Time resolution as a function of bias voltage for NDL #9 and BV170 before irradiation. (b) Time resolution as a function of bias voltage for NDL #10, NDL #9, BV170 after $1.02 \times 10^{15} n_{eq}/cm^2$ irradiation at -30 ^{o}C.

time walk effect could be reduced by using the constant fraction discriminator (CFD) method in frontend electronics and in data analysis. In CFD method, the arrival time of the particle of the CFD is taken to be the time when the pulse passes a specific fraction of the maximum pulse amplitude. The detailed calculation for timing resolution was described in [3]. The CFD fraction for this analysis is chosen to be 50%.

Figure 6 shows the timing resolution as a function of bias voltage for NDL LGAD sensors before and after 1.02×10^{15} $\mathrm{n_{eq}/cm^2}$ irradiation at $-30\,^{\circ}\mathrm{C}$.

The timing resolution of the BV170 after irradiation is 80 ps at -30 °C which is a factor of 2.8 times worse compared with the resolution before irradiation (29 ps). The timing resolution of NDL #9 (#10) after irradiation at -30 °C is 45 (50) ps, which has the potential to satisfy the ATLAS physics requirement in HGTD project. The timing resolution for NDL #9 increased about 2.3 times compared with the best timing resolution before irradiation (20 ps). There's no timing resolution data of NDL #10 before irradiation.

From the results above, the NDL #9 and NDL #10 have a better timing performance than BV170 after irradiation. The doping concentration of the gain layer in NDL #9 and NDL #10 are lower than those of the BV170. NDL #9 and NDL #10 have a higher break down voltage than BV170 as shown in Table 1, and can operate with moderate gain.

4.2. Collected charge

The collected charge for each signal is calculated by dividing the integration of the voltage pulse by the charge-voltage transimpedance of the amplifier. The distribution of the charge collection is fit with Landau distribution to get the charge most probability value (MPV) for a certain bias. We took the MPV to be the collected charge by the NDL LGAD sensors.

Figure 7 shows the collected charges as a function of the bias voltage before and after irradiation up to fluence of 1.02×10^{15} n_{eq}/cm^2 at -30 °C. All NDL LGAD sensors have a collected charge larger than 13 fC before irradiation. The collected charge of BV170 at -30 °C after irradiation is about 4.2 fC, which has the potential to satisfy the requirement of the ATLAS HGTD project (4 fC). The collected charge of BV170 decreases about 3.1 times than the collected charge before irradiation at 20 °C. The collected charge of NDL #9 (#10) after irradiation is about 3 (2) fC, which is slightly lower than the HGTD ASIC requirement. As shown in Figure 4, the total boron dose of the gain layer is similar for BV170 and NDL #9 and NDL #10. However, NDL #9 and NDL #10 have a much wider gain layer, and the peak of doping concentration in the gain layer is about two times lower than BV170. Therefore NDL #9 and #10 are more affected by the acceptor removal effect and have a lower amount of collected charge after irradiation.

In the next prototype run, IHEP and NDL will increase the doping concentration of the gain layer to improve the performance of charge collection after irradiation. While the guard ring design and layout of NDL LGAD prototype will be re-optimized to avoid early breakdown. A thicker epitaxial layer (50 µm) will be used in the next NDL LGAD runs to increase its break

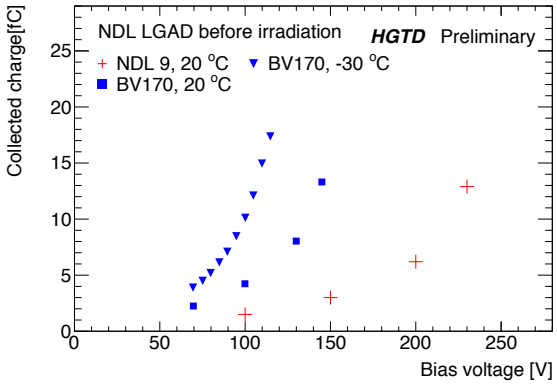

(a)

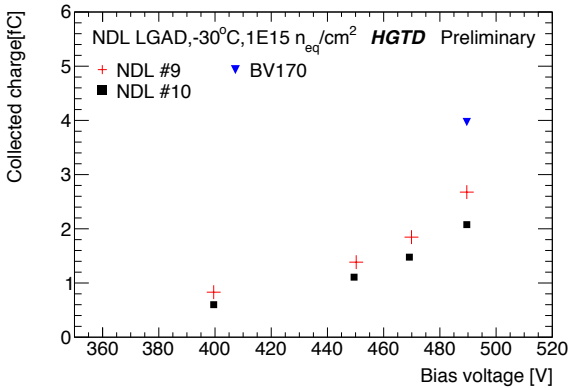

(b)

Figure 7: (a) Collected charge as a function of bias voltage for NDL #9 and BV170 before irradiation. (b) Collected charge as a function of bias voltage for NDL #10, NDL #9, BV170 after $1.02 \times 10^{15} n_{eq}/cm^2$ irradiation at -30 ^{o}C.

down voltage after irradiation. A complete summary of the test results is presented in Table 2.

5. Conclusion

A new LGAD sensor developed by NDL and IHEP, in the context of the HGTD upgrade project of the ATLAS detector for the HL-LHC, has been presented, as well as the results of the radiation hardness of LGAD

Table 2: The timing resolution and collected charge of NDL LGAD sensors before and after irradiated up to fluence of 1.02×10^{15} n_{eq}/cm^2.

Sensor	1.02×10^{15} n_{eq}/cm^2 (−30 °C)		Before irradiation	
	Timing resolution [ps]	Collected Charge [fC]	Timing resolution [ps]	Collected Charge [fC]
NDL #9	45	3	20 (20 °C)	13 (20 °C)
NDL #10	50	2	-	-
BV170	80	4	29 (20 °C) 20 (−30 °C)	13 (20 °C) 17 (−30 °C)

sensor after proton irradiation. All NDL LGAD sensors have excellent timing resolution $20 - 30$ ps and collected charge $13 - 18$ fC before irradiation. After proton irradiation with a fluence of 1.02×10^{15} n_{eq}/cm^2, the NDL BV170 kept a relatively high collected charge (4.2 fC) after irradiation, and its timing resolution is 80 ps; The NDL #9 (#10) obtains a good timing resolution 45 (50) ps, while its collected charge is 3 (2) fC, which is slightly lower than the ATLAS HGTD project requirement. In the next prototype run, IHEP and NDL will increase the doping concentration of the gain layer to improve the performance of charge collection after irradiation. An optimized LGAD layout and guard ring design, as well as a thicker epitaxial layer (50 µm) are also expected in the next runs to increase the breakdown voltage.

Acknowledgement

This work was supported by the National Natural Science Foundation of China (No. 11961141014), the State Key Laboratory of Particle Detection and Electronics (SKLPDE-ZZ-202001), the Hundred Talent Program of the Chinese Academy of Sciences (Y6291150K2), the CAS Center for Excellence in Particle Physics (CCEPP), United States Department of Energy (grant DE-FG02-04ER41286), partially performed within the CERN RD50 collaboration, partially by the Fundamental Research Funds for the Central Universities of China (grant WK2030040100), the Slovenian Research Agency (project J1-1699 and program P1-0135) , MINECO, Spanish Government, under grant RTI2018-094906-B-C21. Thanks to Beijing Normal University for the detector production, and CYRIC for the proton irradiation experiment. Thanks for the contributions from UCSC technical staff and students. Thanks all colleagues involved in these processes.

[1] ATLAS Collaboration, Technical Proposal: A High-Granularity Timing Detector for the ATLAS Phase-II Upgrade (CERN-LHCC-2018-023. LHCC-P-012) (Jun 2018).

[2] G. Apollinari, O. Brüning, T. Nakamoto, L. Rossi, Chapter 1: High Luminosity Large Hadron Collider HL-LHC, CERN Yellow Report (arXiv:1705.08830) (2017) 1–19. 21 p.

[3] N. Cartiglia, et al., Beam test results of a 16 ps timing system based on ultra-fast silicon detectors, Nuclear Instruments and Methods in Physics Research, Section A: Accelerators, Spectrometers, Detectors and Associated Equipment 850 (2017) 83–88.

[4] G. Paternoster, et. al., Developments and first measurements of Ultra-Fast Silicon Detectors produced at FBK, Journal of Instrumentation 12 (2) (2017).

[5] Z. Galloway, et al., Properties of HPK UFSD after neutron irradiation up to 6×10^{15} n_{eq}/cm^2, Nuclear Instruments and Methods in Physics Research Section A: Accelerators, Spectrometers, Detectors and Associated Equipment 940 (2019) 19–29.

[6] G. Kramberger, et al., Radiation effects in Low Gain Avalanche Detectors after hadron irradiations, Journal of Instrumentation 10 (07) (2015) P07006.

[7] M. Ferrero, et. al., Radiation resistant LGAD design, Nuclear Instruments and Methods in Physics Research, Section A: Accelerators, Spectrometers, Detectors and Associated Equipment 919 (2019) 16–26.

[8] Beijing Normal University, Novel Device Laboratory(NDL), `http://www.ndl-sipm.net/indexeng.html` (2020).

[9] Y. Zhao, et al., Comparison of 35 and 50μm thin HPK UFSD after neutron irradiation up to $6 \times 10^{15} n_{eq}/cm^2$, Nuclear Instruments and Methods in Physics Research, Section A: Accelerators 924 (2019) 387–393.

[10] G. Kramberger, et al., Radiation hardness of thin Low Gain Avalanche Detectors, Nuclear Instruments and Methods in Physics Research Section A: Accelerators, Spectrometers, Detectors and Associated Equipment 891 (2018) 68–77.

[11] J. Lange, et al., Gain and time resolution of 45 μm thin low gain avalanche detectors before and after irradiation up to a fluence of 10^{15} n_{eq}/cm^2, Journal of Instrumentation 12 (5) (2017) P05003. arXiv:1703.09004.

[12] E. Peiner, A. Schlachetzki, D. Krüger, Doping Profile Analysis in Si by Electrochemical Capacitance-Voltage Measurements, Journal of The Electrochemical Society 142 (2) (1995) 576.

[13] K. Nagai, H. Takato, Y. Hayashy, Related content Doping Profile Measurement of a Bonded Silicon-on-Insulator Wafer by Capacitance-Voltage Measurements, Japanese Journal of Applied Physics 31 (11A) (1992) L1529.

[14] Z. Yuzhan, UCSC Senior thesis, A study of the timing resolution of ultra fast silicon detectors (2017).